Alloy Formation and CO Adsorption on Bimetallic Ca/Pd(111) Surfaces†

Dmitri I. Jerdev,‡,§ Roel Prins,*,‡ and Bruce E. Koel§

Department of Chemistry, Swiss Federal Institute of Technology, Zurich, CH-8092, Switzerland, and Department of Chemistry, University of Southern California, Los Angeles, California 90089-0482

Received: January 14, 2004; In Final Form: May 5, 2004

Ca films deposited on the surface of Pd(111) were studied by temperature-programmed desorption, X-ray photoelectron spectroscopy (XPS), Auger electron spectroscopy, and low-energy electron diffraction (LEED). Multilayer Ca films desorb at 1180 K, which is much higher than that value for any of the alkali metals. Ca adatoms alloy with Pd at temperatures as low as 700 K. Annealing sub-monolayer Ca films at 1100 K reproducibly formed two well-ordered surface structures with (2×2) and $(\sqrt{3}\times\sqrt{3})$R30° Ca/Pd(111) unit cells depending on the amount of Ca deposited on the Pd(111) substrate. Chemical shifts of Ca XPS peaks indicate that these ordered structures are correlated to the formation of Ca−Pd alloys. The presence of Ca at the Pd(111) surface increases the CO adsorption energy and causes a 110-K shift of the CO thermal desorption peak to a higher temperature than from a clean Pd(111) surface. This Ca−Pd−CO interaction is so strong that it drives Ca out of a Ca−Pd alloyed layer to the overlayer upon CO adsorption, which is evident from the disappearance of the characteristic LEED pattern of the alloy. This migration of Ca atoms occurs without oxidation of Ca. These observations are discussed with reference to possible active phases in Ca-modified, supported Pd catalysts for methanol synthesis and the special nature of Ca over alkali metal promoters for this catalysis.

Introduction

Alkali and alkaline-earth additives are commonly added to transition metal supported catalysts as "promoters" to increase the activity and/or selectivity of the catalyst. One of the first patents described how potassium modified an Fe catalyst to greatly increase the yield of ammonia in ammonia synthesis. Since then, alkali and alkaline-earth metals have been used to modify catalysts for a number of important industrial processes, e.g., Fischer−Tropsch and alcohol synthesis, which are indispensable in today's chemical industry.

The aim of catalytic science in recent years has been to prepare and modify supported catalysts to achieve high selectivity to desirable products. Although there are a number of ways to influence the selectivity of a catalyst, the preparation of selective catalysts is a difficult task that remains the "art of catalysis" to a large extent. To find a systematic approach for solving this problem, it is useful to investigate catalysts that undergo a well-pronounced selectivity improvement as a result of modification by a particular additive. One example of such a situation was reported for a Pt catalyst in the hydrogenation of acetylene to ethylene.[1] A large amount of ethane is formed on a pure Pt catalyst; however, the selectivity increased considerably (while retaining the conversion rate) when the Pt surface was electrochemically promoted by 0.02-monolayer (ML) Na delivered from a β-alumina solid electrolyte. Another case where such selectivity improvement has been reported is CO conversion over supported Pd catalysts.[2] In this system, the addition of Ca to the catalyst improved the selectivity to methanol formation from 42 to 99%. Although Pd catalysts can hardly compete with the industrial Cu/ZnO catalyst used currently, as far as price is considered, the Ca-promoted Pd/SiO_2 catalyst was chosen in this work as a model system to investigate the nature and mechanism of such a dramatic change in catalytic properties caused by addition of a promoter.

Other researchers reported[3] that SiO_2-supported Pd catalysts have high activity and selectivity in the hydrogenation of CO to CH_3OH and attributed this to the fact that Pd adsorbs CO molecularly.[4,5] However, Pd black and unsupported Pd catalysts show poor performance for CO to methanol conversion.[6] Furthermore, the catalytic properties of SiO_2-supported Pd catalysts depend strongly on the commercial supplier of the support.[7] This suggested that the high activity of Pd catalysts made from commercial SiO_2 arises from contaminants that are always present in industrial-grade SiO_2.[2] To prove this, many promoters were tested and characterized for their effects on this catalyst.[2] Among the most efficient promoters were CaO, Li_2O, FeO_x, and La_2O_3. Among the alkali metals, only Li had a reasonable promoting effect whereas Na, K, Rb, and Cs improved the activity of the catalyst to a much smaller extent. All of the alkaline-earth metals were fairly good promoters and greatly improved the yield of methanol. The best result in terms of selectivity to methanol in this group was obtained for Ca. La was found to be the most effective promoter of the activity, or turnover frequency, but it is inferior to Ca because of a significant rate for the side reaction to methane. Recent studies have investigated Ca as a promoter in even more detail.[8] The addition of Ca to a SiO_2-supported Pd catalyst promoted methanol formation to values very close to those typical of the industrially used Cu/ZnO catalyst. The maximum promotional effect was obtained at a Ca/Pd molar ratio of 0.1 used in the catalyst preparation.

The promotional effect of Ca to increase the selectivity of the catalyst to form methanol may arise from palladate forma-

† Part of the special issue "Gerhard Ertl Festschrift".

* To whom correspondence may be addressed. E-mail: roel.prins@chem.ethz.ch.

‡ Swiss Federal Institute of Technology.

§ University of Southern California.

10.1021/jp049817v CCC: $27.50
Published on Web 06/18/2004

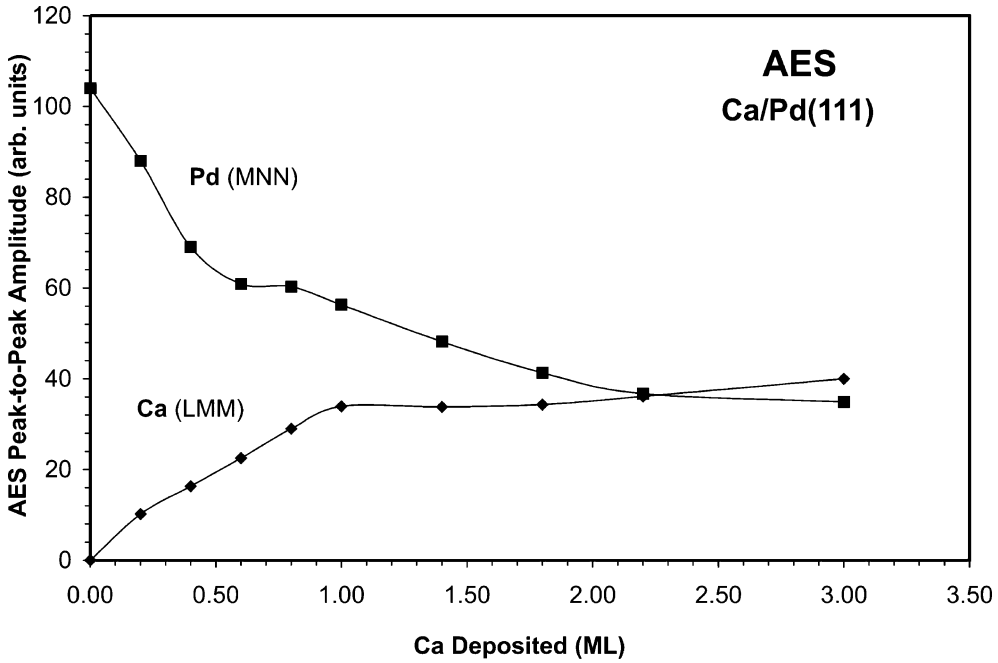

Figure 1. AES data for Ca deposition on a Pd(111) surface at 330 K. An incident beam energy $E_p = 3$ keV was used.

tion. Substances such as $CaPd_3O_4$ have been reported and form under conditions similar to those used for catalyst activation.[9] Another rationale could be the surface modification of Pd particles by Ca adatoms or formation of Ca−Pd alloy phases. No surface-science literature is available concerning such interactions or the chemistry of such surfaces. To comment on this rationale, we conceived the present study to investigate the structure and chemistry of bimetallic Ca−Pd surfaces, specifically aimed at probing Ca−Pd surface alloying, thermal stability of Ca−Pd surfaces, and CO adsorption on Ca-modified Pd(111) surfaces.

We might expect the interactions in this system to resemble those of the well-studied alkali−transition-metal systems. The unique properties of alkali and alkaline-earth elements result from their location in the periodic table and the relatively high position of the metal Fermi level. This results in facile donation of electrons to transition metals so that alkali and alkaline-earth adatoms exist on transition-metal surfaces in a partially ionic form. Donation of electron density from the admetal to the substrate causes a decrease in the substrate work function,[10−13] and this effect is utilized in the production of cathodes for vacuum devices. The presence of highly charged surface entities causes polarization of surrounding molecules and affects molecule−surface charge transfer and bond strength. This affects bond activation and changes the stability of adsorbed moieties.[14] Surface alloy formation in the comparable Li−Pd system was proposed as an explanation for the high activity for the formation of methanol from synthesis gas over a Li-promoted Pd/SiO_2 catalyst.[15]

Experimental Section

Preparation of the Ca/Pd(111) surfaces investigated was done in an ultrahigh vacuum (UHV) chamber[16] equipped with facilities for X-ray photoelectron spectroscopy (XPS), low-energy ion scattering (LEIS), Auger electron spectroscopy (AES), and low-energy electron diffraction (LEED) at a background pressure of 2×10^{-10} Torr. The Pd(111) surface was cleaned by cycles of Ar^+-ion bombardment at 2 keV (3 μA, 5 min) at 350 K and subsequent annealing in a vacuum to 1200 K. Surface cleanliness was monitored routinely by XPS, and no impurities above 0.5 atomic % were detected by either XPS or AES.

A Ca doser was constructed by using a piece of metallic calcium (Alfa Aesar, 99.5% pure) placed into a tantalum boat that was heated resistively. Ca was evaporated onto the Pd(111) surface through a hole (~1 mm diameter) in the cover of the Ta boat. During Ca evaporation, the background pressure rose to 9×10^{-10} Torr, but experiments were carried out only when C, O, and S impurities in the film were below XPS detection levels of 0.03, 0.01, and 0.02 ML, respectively.

XPS spectra were taken with a Mg Kα source (300 W, 15 kV) using an analyzer pass energy of 29.35 eV for Pd and Ca and 46.95 eV for C and O. All scan times were on the order of a few minutes. The angle between the surface normal and the XPS analyzer input lens axis was 45°. Binding energies are referenced to the Pd $3d_{5/2}$ peak at 334.85 eV BE for clean Pd(111).

Results and Discussion

Ca−Pd Alloy Preparation and Characterization. AES and XPS were used to calibrate the Ca deposition rate and characterize the Ca film growth. Figure 1 shows the change in Pd and Ca AES signals with the amount of Ca deposited at a constant Ca doser current onto the Pd(111) substrate at 300 K. The Ca signal exhibits a sharp break at a particular point, referred to hereafter as the time required to deposit 1 ML of Ca (this interpretation is supported by work-function measurements shown later). Figures 2a and 3a show the Pd 3d and Ca 3p XPS spectra, respectively, within the Ca coverage range from 0 to 1 ML. Chemical shifts of these peaks will be discussed below, but for now we address the intensity changes in these spectra.

The increase in Ca and decrease in Pd signals in AES and XPS within a layer-by-layer growth model can be calculated using values for the appropriate electron inelastic mean free paths (λ) in a Ca film. This calculation provides an estimate of the Pd signal attenuation expected for deposition of 1-ML Ca on the surface. By use of λ(340 eV) = 15 Å in a Ca film for the Pd(MNN) Auger electrons, calculated as described in ref 17, a thickness for the monolayer Ca film of 3.9 Å, and an emission takeoff angle of 45°, one predicts the attenuation of

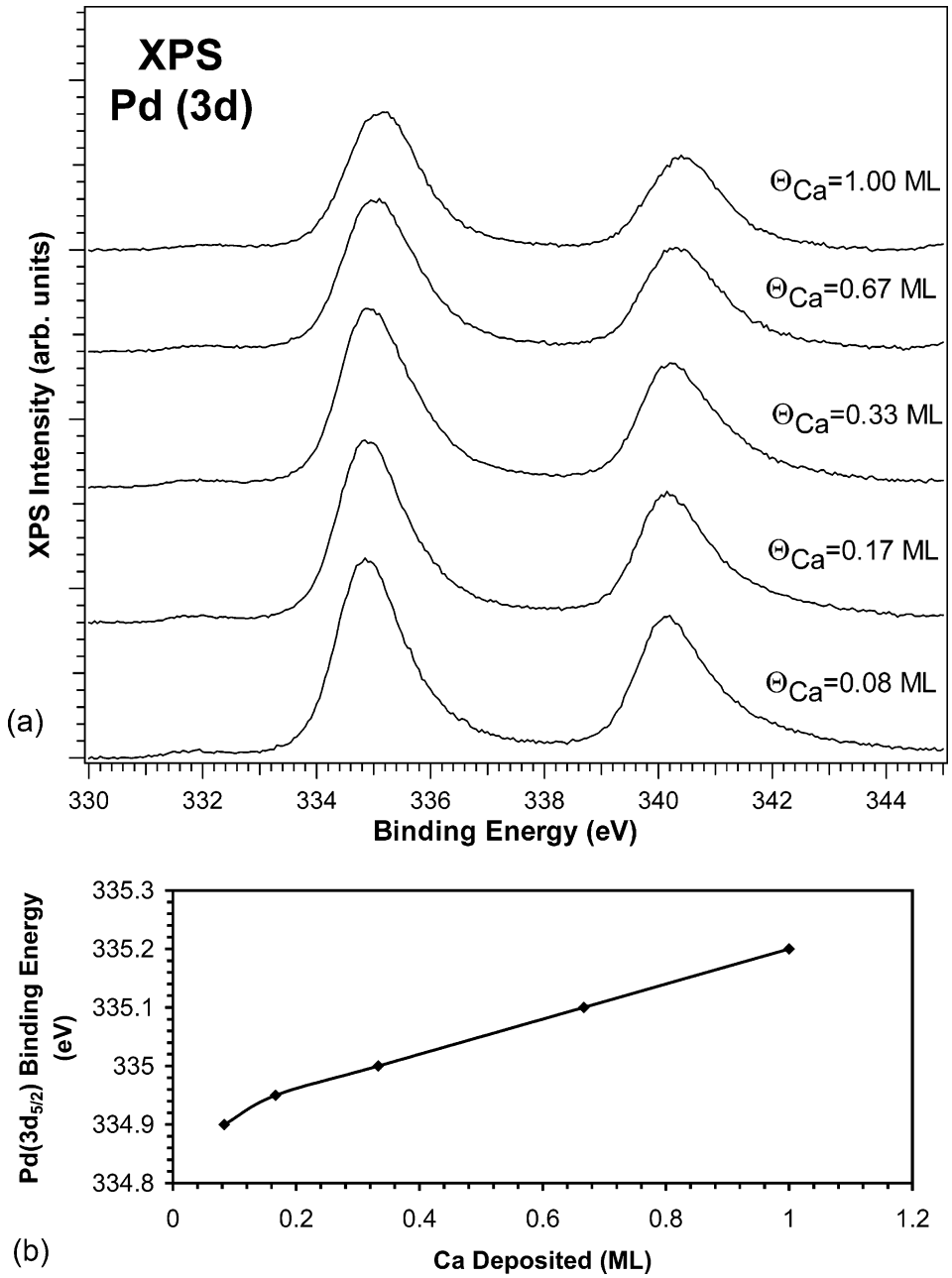

Figure 2. (a) Pd 3d core levels in XPS for several Ca films on Pd(111). (b) Shift in Pd $3d_{5/2}$ XPS line with Ca coverage.

the Pd(MNN) AES signal to be 0.62 relative to the signal from the clean surface. A similar calculation using the Pd 3d XPS peak and λ(905 eV) = 30 Å predicts an attenuation of the Pd 3d signal by a 1-ML Ca film of 0.87 relative to the signal from the clean surface. In both AES and XPS, the dose unit that was denoted as 1-ML Ca (as defined above) resulted in a larger decrease in the Pd signal (0.57 in AES and 0.80 in XPS) relative to the clean Pd(111) surface than was expected. While this could mean that the amount of Ca deposited is larger than we report, several other factors could influence these results such as intensity variations with emission angle, influence of Ca on the Pd Auger line shape, or a decreased value of λ in the Ca monolayer. In such studies, we typically rely on He^+ LEIS for calibrating surface coverages and film growth, and this possibility was investigated. However, as expected for analysis of alkali and alkaline earth adatoms, the LEIS spectrum revealed a very weak peak for Ca (results not shown). This situation results from very effective charge exchange between the incident ion beam and surface for such systems.[18] Therefore, LEIS was not further used in this study.

XPS also showed that deposition of Ca on the Pd(111) surface was accompanied by a strong electronic interaction between Ca and Pd. Significant shifts in both Pd 3d and Ca 3p XPS peaks with Ca deposition are shown in Figures 2b and 3b, respectively. In synchrotron-based studies of Li growth on the Mo(110) surface,[19] a shift was reported of the Mo valance d states to higher binding energy and Li 1s level to lower binding energy with increasing Li coverage. This phenomenon was attributed to the change in potential induced in the boundary region. In our case, this shift occurred gradually with Ca coverage without detectable broadening of the Pd 3d peaks. Furthermore, we took difference spectra in an attempt to identify any small, additional, chemically shifted Pd peak distinct from the bulk Pd emission. These difference spectra and several curve-fitting approaches failed to identify any such "second" Pd peak; however, we found that the high binding energy tail of the Pd 3d peaks, where one

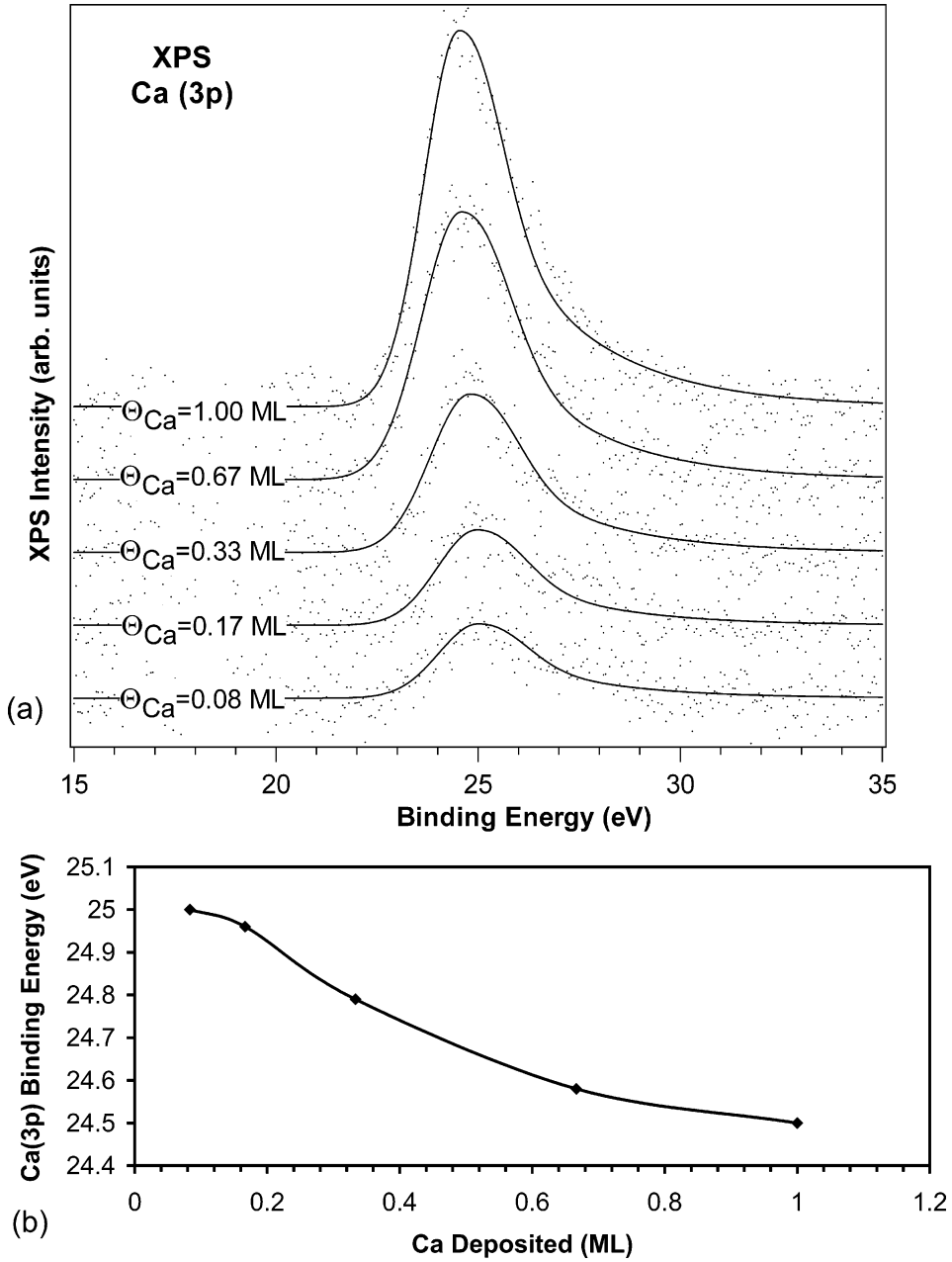

Figure 3. (a) Ca 3p core levels in XPS for several Ca films on Pd(111). (b) Shift in Ca 3p XPS line with Ca coverage.

expects to see many-electron effects, was increased in relative intensity in the presence of Ca.

The shift of the Ca 3p XPS peak to lower binding energy with increasing Ca coverage results from changing the character of Ca on the surface from mostly ionic at low coverage to mostly metallic for thicker Ca films.

A 2-ML Ca film deposited on Pd(111) at 320 K was heated and probed by XPS to characterize the stability of the Ca film and alloy formation. In these experiments, the Ca film was sequentially annealed to 1000 K in steps, with a 10-s pause at each temperature, and Ca 3p and Pd 3d XPS spectra were taken at 320 K after each annealing step. The Pd 3d XPS spectra and the changes in the XPS intensities during this experiment are shown in Figure 4. The positions of the XPS peaks of both elements also changed. The Pd 3d XPS peaks after deposition of 2-ML Ca are shifted significantly (+0.4 eV) from those of clean Pd(111) (Figure 4a). This shift gradually decreases with annealing and practically disappears by 800 K, despite the significant Ca concentration (>1 ML) that remained. As mentioned above, this is induced by the altered potential in the Ca−Pd interface region. As the temperature increased, the boundary between Ca and Pd becomes less pronounced because of interdiffusion or alloying of these two metals. This results in formation of a more continuous, homogeneous alloyed region that has no abrupt interface field and thus the Pd 3d core level shows no chemical shift. In this region, the position of the Ca 2p XPS peak also does not change significantly.

Figure 4b shows the decrease in the intensity of the Ca signal and increase in the Pd signal as the temperature is raised. From 330 to 950 K, these changes are attributed to interdiffusion, i.e., alloying, of Ca and Pd. Above 1000 K, the rate of disappearance of Ca increases rapidly with temperature at least in part due to evaporation of Ca from the surface. At a final temperature of 1280 K, the Ca 3p intensity had decreased to about 16% of its initial value for the 2-ML Ca film prior to annealing, which is equivalent to about 0.3-ML Ca.

Ca films deposited on the Pd(111) surface at 320 K did not exhibit any LEED pattern other than the (1 × 1) pattern of

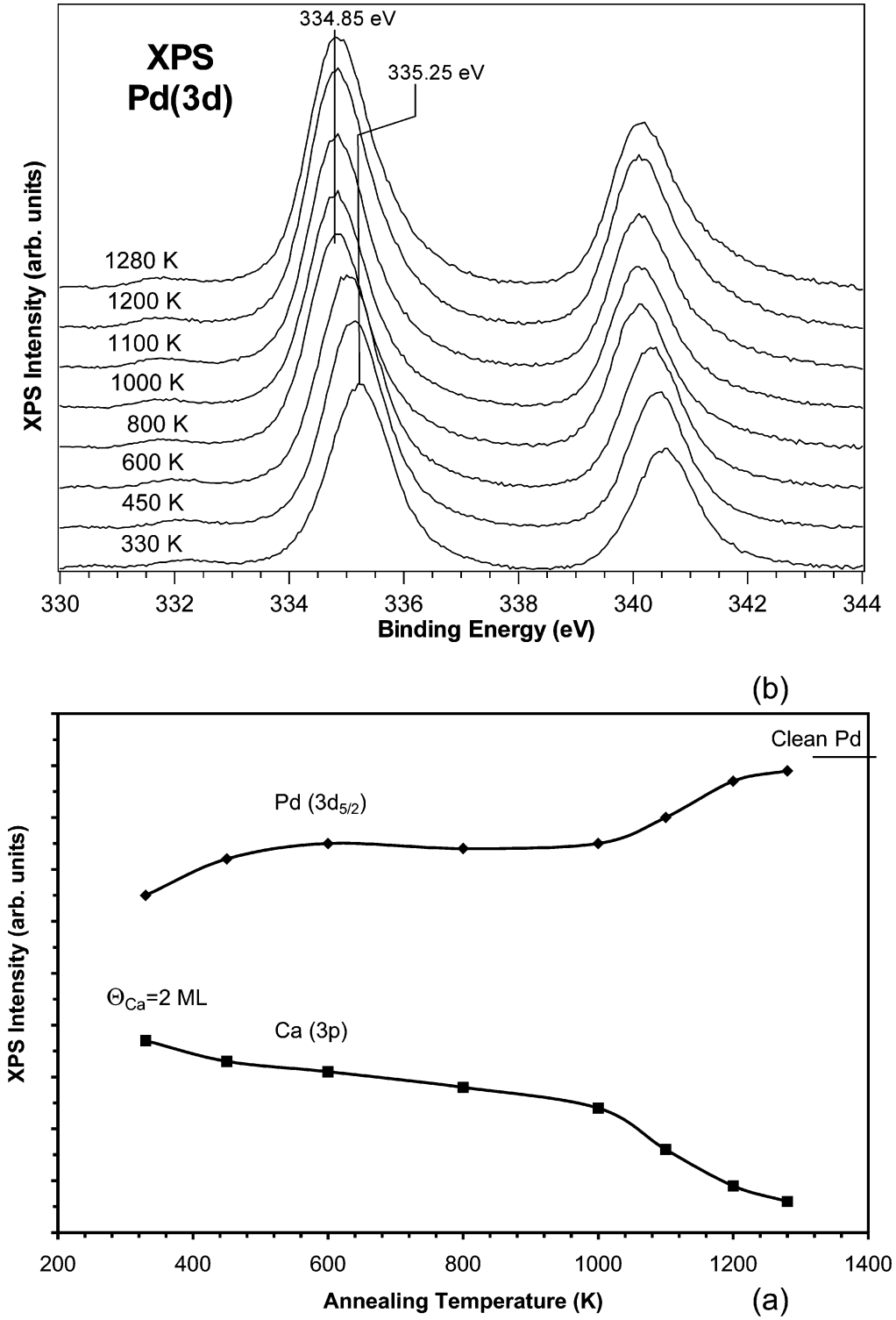

Figure 4. Studies of the influence of annealing on a 2-ML Ca film on Pd(111). (a) Pd 3d core level in XPS; (b) Pd and Ca coverage deduced from XPS signals. The annealing time was 20 s at each temperature.

Pd(111), which disappeared with increasing Ca deposition. However, new spots appeared to give well-defined LEED patterns when Ca films were annealed to 700−1100 K. Depending on the initial amount of deposited Ca, two patterns were obtained: a (2 × 2) structure for $\Theta_{Ca}^{init} = 0.4$ and a $(\sqrt{3}\times\sqrt{3})$R30° structure for $\Theta_{Ca}^{init} = 0.9$ ML. These patterns are shown in parts a and b of Figure 5, respectively. Both of these surfaces are characterized by XPS core-level peaks for Ca 3p at 24.35 eV BE and Pd(3d) 334.85 eV BE. This Pd 3d peak is unshifted from the clean Pd(111) surface value. We believe that alloy formation rather than overlayer ordering is responsible for these ordered structures for two primary reasons: (i) the high temperature necessary to form the LEED patterns and (ii) the absence of the strongly shifted Pd 3d peak that was evident for all Ca films upon deposition on Pd(111) at 320 K. We propose that the annealing of Ca films to 1000 K leads to interdiffusion and formation of an ordered alloy, i.e., intermetallic compound. Primitive unit cells with incorporated Ca atoms occupying Pd lattice positions in the surface layer would predict a surface Ca coverage of 0.25 and 0.33 ML,

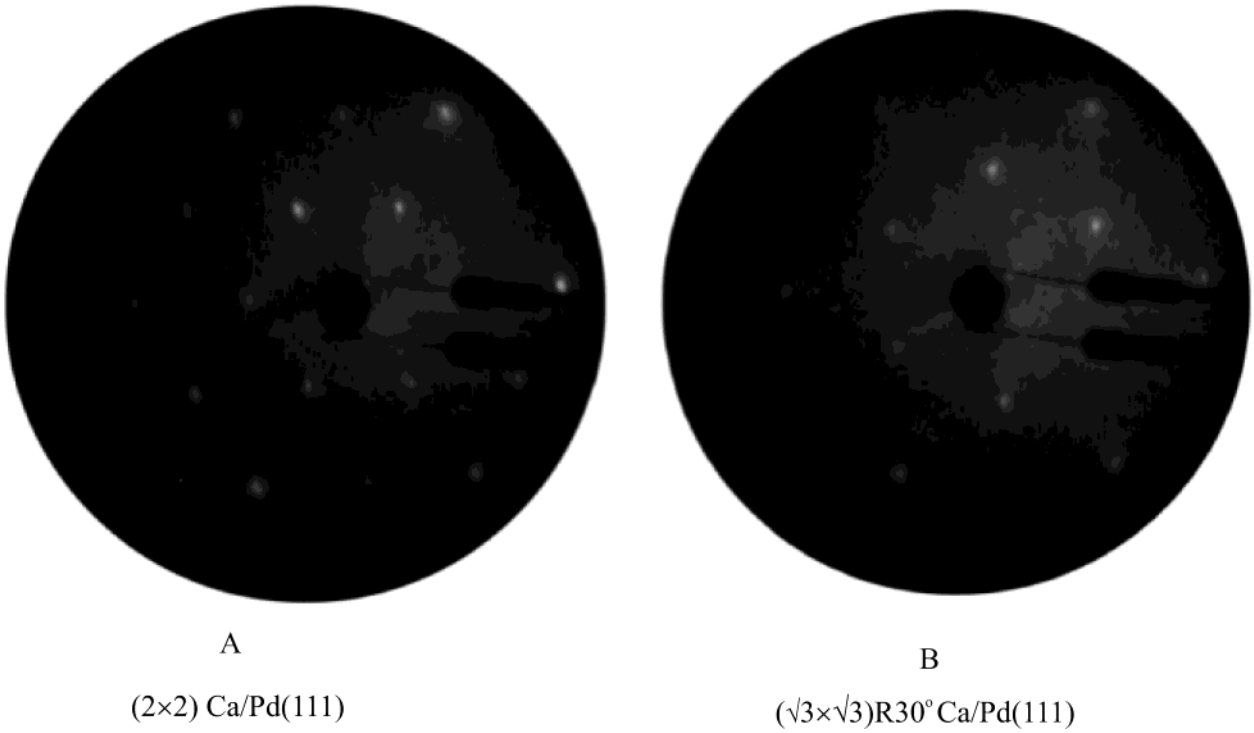

Figure 5. LEED patterns obtained for the (a) (2 × 2) and (b) ($\sqrt{3}\times\sqrt{3}$)R30° Ca/Pd(111) alloys after annealing of 0.4- and 0.9-ML Ca films on Pd(111) for 20 s at 1100 K. An incident beam energy $E_p = 60.0$ eV was used for both images.

respectively, for the (2 × 2) and the ($\sqrt{3}\times\sqrt{3}$)R30° Ca/Pd(111) surface alloys. These values are consistent with the estimations of the Ca concentration using AES and XPS.

These observations demonstrate that Ca deposition and the subsequent thermal stability of the film differs considerably from that of alkali metals on transitional metal surfaces. The surface mobility of alkali adatoms usually is sufficient to form ordered superstructures due to dipole−dipole repulsion[20] even at low temperatures (~300 K). Alkali adatoms in such overlayers are so mobile that they are often referred to as a 2D lattice gas. A number of different superstructures have been reported for Na/Ru(001),[21] Cs/Rh(100),[22] K/(Pt(111),[23] and K/Ni(111),[24] depending on the adatom coverage and temperature. In the case of Ca, the surface mobility of Ca adatoms at room temperature is sufficiently low such that the film is disordered even in the presence of strong dipole−dipole repulsive interactions. Alloying has not typically been reported for alkali metal−transition metal systems. This may be due to the relatively small barrier for thermal evaporation compared to interdiffusion in these systems. Ca films are stable to much higher temperatures than those of alkali metals, and large interdiffusion barriers can be surmounted before desorption of Ca into the gas phase.

The change in work function was measured as a function of the amount of Ca deposited on Pd(111) at 320 K. This is a useful probe of the ionic character of Ca in the adlayer. No previous studies of Ca deposited on transitional metals are available, but we can expect some similarity with the behavior observed for alkali metal adsorption.

The work function of the surface was measured by using the onset for secondary electron emission. An incident beam of low energy electrons (100 eV) was directed at the surface, and the kinetic energy spectrum of electrons emerging from the sample was recorded using the SCA operated at 29.6-eV pass energy (0.45 eV resolution). The threshold energy for emission was determined as the position of the sharp increase in the number of electrons as judged using the first 10% or so of intensity of the secondary electron emission distribution. This method readily allows measurement of work-function changes. It is more difficult to make absolute determinations of work-function values, and we use a reported value of the work function of clean Pd (111) of 5.12 eV.[25] Figure 6 provides the results of these measurements.

The steep work-function decrease found at low Ca concentrations corresponds to the region where electrons are donated substantially from Ca adatoms to the substrate. In this region, Ca atoms transfer most of the 3s electron density to Pd and the bond between Ca and the surface is mostly ionic.[26] This extensive charge transfer establishes an electrostatic field that is the primary contribution to the observed change in the work function. As in cases of alkali adsorption, we observed a well-pronounced minimum in the work-function curve vs admetal coverage that occurs in Figure 6 near 0.7-ML Ca. The decreasing influence of added Ca and the changes that occur in the region of this minimum result from decreasing charge transfer from Ca to the substrate because of the increasing energy required to charge the adlayer. This leads to depolarization within the adlayer and gradual conversion of Ca−Pd bonding from ionic to metallic. A 2-ML-thick Ca film on Pd(111) was characterized by a work function of 2.6 eV, which is close to a value of 2.87 eV for Ca metal.[25] As a final note, the nonmonotonic dependence of the work-function change at low Ca concentrations observed in Figure 6 has also been seen in several cases of alkali metal adsorption.[26]

The thermal stability of Ca films deposited on Pd(111) was also analyzed using Ca TPD. Ca films of different thickness were annealed to 1300 K while recording the signal from the quadrupole mass spectrometer at 40 amu corresponding to Ca desorption. The resulting curves are shown in Figure 7. The desorption behavior of Ca from Pd(111) varies strongly in the region of initial Ca coverages that was explored, ranging from multiple Ca desorption peaks to a single, zero-order desorption peak for the 5-ML Ca film. In all TPD experiments, the

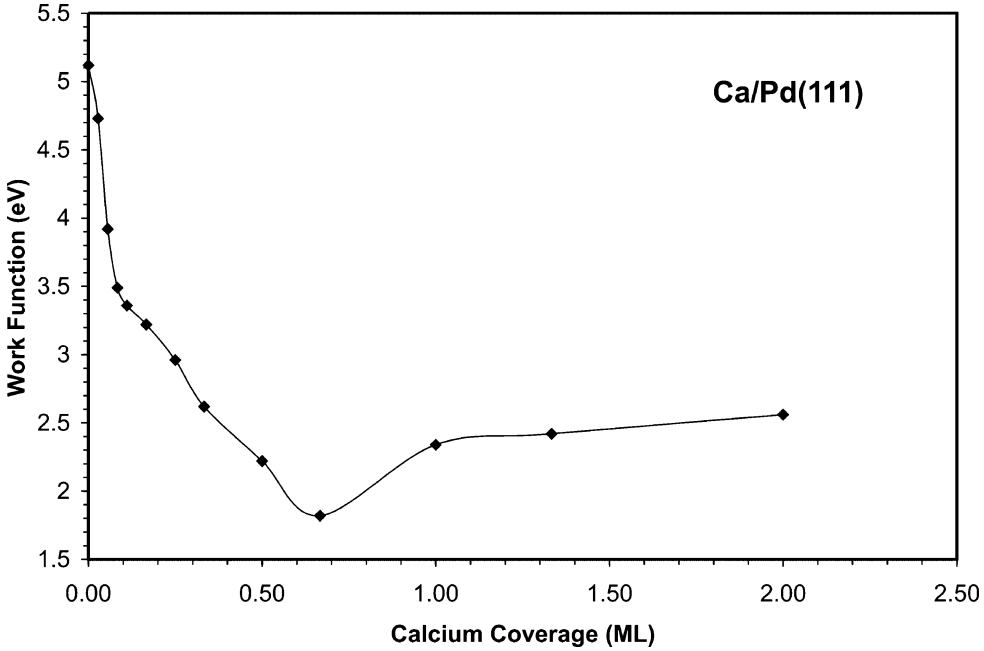

Figure 6. Work-function change, $\Delta\phi$, vs Ca surface concentration.

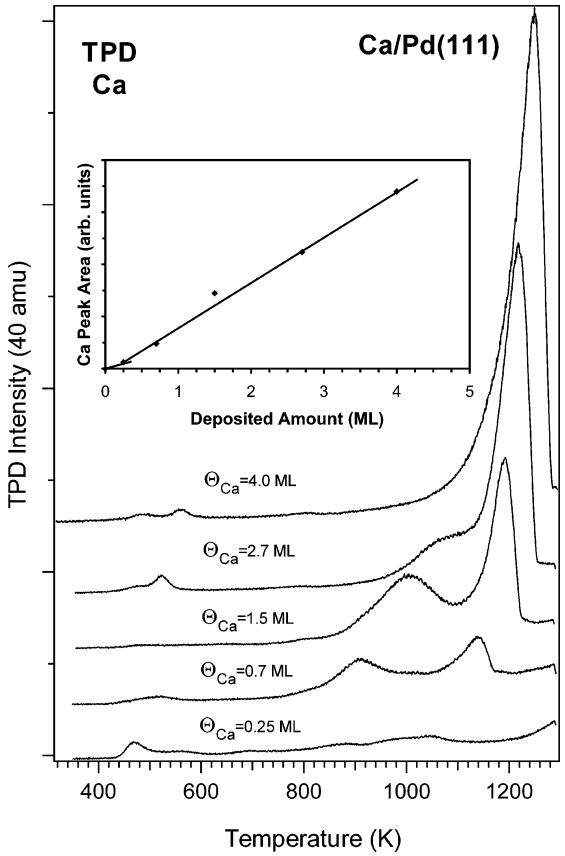

Figure 7. Ca TPD from different thicknesses of Ca films on Pd(111).

decomposition temperature of the (2 × 2) Ca/Pd(111) alloy could not be reached because of the temperature limitation set by the chromel−alumel thermocouple. Thus, the characteristic LEED pattern for this alloy was observed upon completion of all of the TPD experiments. Formation of this alloy phase consumes some of the initially deposited Ca, and this is responsible for the small induction period observed in a plot of the amount of Ca desorbed from the surface (calculated from TPD curve areas) vs the initial amount of deposited Ca, as shown in the inset of Figure 7.

Two Ca peaks were observed during Ca desorption from the Pd surface. We attribute these two peaks to desorption of Ca from two, Ca−Pd surface alloy phases: (2 × 2) and ($\sqrt{3}\times\sqrt{3}$)R30° Ca/Pd(111). The number of Ca−Pd bonds for each Pd atom in the surface layer differs between the two alloy structures, and this alters the Ca desorption energy. The higher temperature Ca desorption peak, which is first observed at 1060 K for 0.25-ML Ca and gradually shifts to 1250 K at the highest coverages, is due to desorption of Ca from metallic adislands at the surface of the (2 × 2) alloy. This alloy structure still possesses pure-Pd, 3-fold sites, and the surface binds Ca adatoms tightly. The low-temperature peak is due to desorption of Ca from metallic adislands on the ($\sqrt{3}\times\sqrt{3}$)R30° Ca/Pd(111) alloy. This alloy has a larger number of Ca−Pd bonds for each Pd atom in the surface of the alloy and only possesses pure-Pd, 2-fold sites. This decreases the adsorption energy of Ca in adlayers on the surface, and Ca desorbs at lower temperatures than on the (2 × 2) alloy. If Ca adatoms in these layers were substantially charged, one would expect the Ca TPD peak to broaden or shift to lower temperature with increasing Ca coverage because of mutual depolarization and weakening of the Ca−Pd bonding interaction. We explain the observed shift to higher temperatures as due to the formation of nearly metallic adislands with increasing average diameter on top of the alloy surfaces. Small diameters of these islands have an increased Ca vapor pressure by the Kelvin effect, and this results in Ca desorption peaks that shift to higher temperatures with increasing Ca concentration, which increases the average island size. Eventually, for thick films of deposited Ca, desorption of Ca from these states becomes undistinguishable from Ca sublimation from the thick Ca film.

Several observations support this assignment. First, a leading-edge analysis[27] of the TPD curve from the 5-ML Ca film gives an estimate for the Ca sublimation energy of 41.4 kcal/mol, which is in a good agreement with a value reported for solid Ca (42.5 kcal/mol).[28] This supports our assignment of the high-temperature TPD peak as originating from sublimation from a metallic Ca film rather than diffusion of Ca from the subsurface region. Second, LEED observations were obtained during a heating ramp that was identical to that used in TPD, which was

interrupted sequentially at several temperatures to observe the LEED pattern. These observations were consistent with our model described above. Deposition of a 0.7-ML Ca film on Pd(111) at 300 K resulted in a diffuse (1 × 1) pattern. Spots arising from the ($\sqrt{3}\times\sqrt{3}$)R30° structure first appeared at 700 K, and the pattern sharpened and the surface appeared well ordered at 800 K. Heating to 900 K caused a mixed pattern to appear arising from both (2 × 2) and ($3^{1/2} \times 3^{1/2}$)R30° spots. The ($3^{1/2} \times 3^{1/2}$)R30° spots were removed by heating to 1000 K, leaving a sharp (2 × 2) pattern.

The ($\sqrt{3}\times\sqrt{3}$)R30° alloy is significantly less stable than the (2 × 2) surface alloy. The desorption of Ca and appearance of (2 × 2) LEED spots at 900 K from the 0.7-ML Ca film provides a rough estimate of the binding energy of Ca in this alloy of 50−56 kcal/mol, assuming first-order desorption and a pre-exponential factor of 10^{13} s^{-1}. The (2 × 2) surface alloy is significantly more stable than this alloy and multilayer Ca films. The (2 × 2) alloy can be annealed at 1100 K for several minutes or heated to 1280 K during TPD without losing the (2 × 2) LEED pattern. This sets a lower boundary for the Pd−Ca bond dissociation energy in this alloy of 83−86 kcal/mol, assuming first-order desorption in a peak at 1280 K and a typical pre-exponential factor of 10^{13} s^{-1}. The heat of formation of bulk Pd−Ca alloys is 11−16 kcal/mol,[29] and this means that Ca desorption from the alloy occurs at significantly higher temperatures than from multilayer Ca films.

The high temperatures needed for Ca desorption are indicative of the high stability of Ca on the surface of Pd. This could play a crucial role in the promotional activity of Ca on the Pd catalyst. To be effective, a promoter must be thermally stable at the surface, at least, and this is not the case in a number of alkali/transitional-metal systems. For example, K and Na desorb from the surface of Pt below 500 K,[23] similar to Na from Ru.[21] Among the alkali metals, only Li desorbs at high temperatures of 800 K, as reported for Li on Ru(001).[30] This trend becomes even more relevant to the stability of the alkali species at the surface in the presence of CO if we consider co-desorption of the alkali metals with CO. Na and K show a co-desorption peak at a temperature as low as 650−670 K,[31−33] while this peak for Li appears at 840 K.[30] This could explain why Li is the only metal to promote a methanol formation over supported Pd, while other alkali metals have only a marginal effect.[2] The stability of these alkali metals on the Pd surface would probably increase if they were oxidized. However, the nature of the alkali as a promoter depends to a great extent on its ability to donate electrons to the underlying metal substrate. This ability will be reduced in the case of oxide formation, which is necessary for its stabilization. Furthermore, even if an alkali oxide forms, Pd dissociatively adsorbs hydrogen and could reduce those oxides in situ. The alkali metal formed by this reduction could leave the surface at a typical reaction temperature (550 K), which is close to that required for alkali metal desorption.

CO Adsorption Study on Bimetallic Ca/Pd(111) Surface. CO was used as a convenient probe of reactivity of bimetallic Ca/Pd(111) surfaces. Chemical reactions of CO are also of direct relevance to methanol synthesis catalysis. CO adsorption was studied by means of TPD and XPS on the surfaces of the (2 × 2) as well as ($\sqrt{3}\times\sqrt{3}$)R30° Ca/Pd(111) surface alloys. Measurements were also performed on Pd(111) for comparison. The CO coverage on all surfaces was calibrated relative to the saturation CO coverage obtained by dosing CO on the Pd(111) surface at 300 K, which is reported to be 0.55 ML.[33,34]

Two types of CO TPD experiments were performed. First, we monitored CO desorption from the (2 × 2) alloy surface as the CO exposure was varied. This surface was chosen because it is the most stable surface, with a constant Ca concentration of 0.25 ML during the TPD experiment. In a second set of experiments, we used saturation doses of CO to obtain CO TPD curves for several concentrations of Ca at the Pd(111) surface.

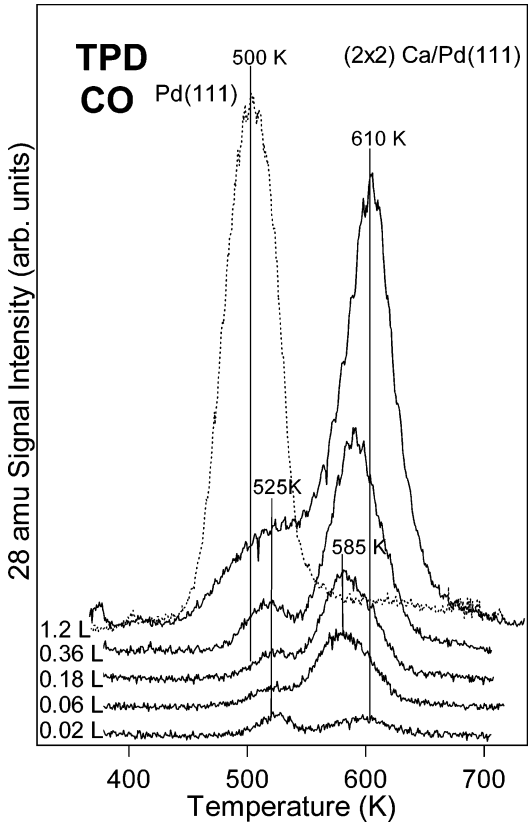

Figure 8. CO TPD from (2 × 2) alloy surfaces that were exposed to different amounts of CO.

Data from the first series of TPD experiments are shown in Figure 8. CO TPD from the Pd(111) surface (indicated by dashed curve) is characterized by a single CO peak at 500 K. CO TPD from the (2 × 2) alloy indicates the existence of two CO adsorption states. The lower-temperature desorption peak may be associated with CO binding to sites characteristic for the clean Pd(111) surface. Most adsorbed CO desorbs from the surface of the (2 × 2) alloy at higher temperature in a peak at 585−610 K. CO adsorption on all of these surfaces was reversible, and no other products were detected in TPD, and no surface carbon was detected by XPS upon completion of the TPD scan. Small amounts of oxygen are difficult to detect by XPS because of the interference from the Pd $3p_{3/2}$ core level.

The CO desorption peak at 500 K from Pd(111) corresponds to a CO desorption activation energy of 31 kcal/mol, assuming first-order desorption and a typical pre-exponential factor of 10^{13} s^{-1}. By use of the same analysis, the CO desorption peak at 610 K from the bimetallic Pd−Ca surface corresponds to a CO desorption energy of 38 kcal/mol.

Adsorption of CO on the (2 × 2) alloy caused the characteristic (2 × 2) LEED pattern to disappear. This LEED pattern could be restored by subsequent annealing to 1100 K. This indicates that CO adsorption occurs with Ca abstraction from the alloy into the adlayer. This occurs without CO dissociation as noted above and was confirmed by irreversible loss of the LEED pattern following intentional oxidation of the alloy using O_2 exposures. This relocation of Ca into the adlayer results in the formation of a charged Ca overlayer that stabilizes adsorbed

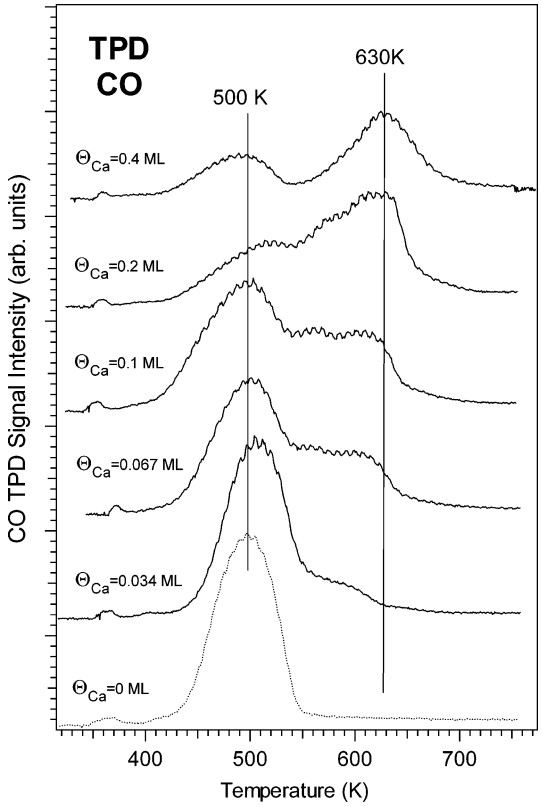

Figure 9. CO TPD after saturation doses of CO were given on Pd(111) surfaces containing varying Ca coverages.

CO. This increase in the CO surface bond strength drives this adsorbate-induced reconstruction and causes CO to desorb at a higher temperature than on clean Pd(111).

We also investigated CO adsorption and desorption on the $(\sqrt{3}\times\sqrt{3})$R30° Ca/Pd(111) alloy (results are not shown). A saturation CO exposure on this alloy at 320 K caused the LEED pattern to change to a (2 × 2) and gave a subsequent CO TPD trace similar to the top alloy curve in Figure 8.

CO TPD curves following CO saturation doses on surfaces containing different Ca concentrations are shown in Figure 9. In these experiments, Ca was deposited on the clean Pd(111) surface at 300 K and a saturation CO dose (3 L) was given immediately after Ca deposition. No annealing was done prior to obtaining the CO TPD curve to ensure that no loss of surface Ca occurs from diffusion into the subsurface and to ensure that we are probing the influence of a Ca adlayer on CO adsorption and desorption kinetics. As shown in Figure 9, two CO desorption peaks could be identified in this series. The first peak, apparently associated with relatively unmodified Pd(111) domains, occurs at 500 K. A high-temperature peak near 630 K arises from desorption of CO bound at Ca-modified sites. The area of this peak and the amount of CO of this type increases with Ca coverage. The broad desorption profile between these two peaks may indicate the influence of the varying local Ca concentration to cause different CO adsorption energies.

Deposition of Ca on the Pd(111) surface initially creates a network of charged Ca adatoms, each of which modifies several Pd atoms in its vicinity. This results in the appearance of a new CO desorption state, which increases in size with increased Ca coverage. Each Ca adatom can modify several Pd atoms, and thus the CO desorption state associated with Ca modification is visible even at very small Ca concentrations. In an analogous system, photoemission of adsorbed xenon (PAX) studies of K adsorbed on Ru(001) determined that each K adatom strongly decreased the work function within an area of 8 Å in diameter.[36] In Figure 8 at $\Theta_{Ca} = 0.4$ ML, CO desorbs in two separate peaks attributed to CO adsorbed on modified and unmodified Pd regions. The electrostatic repulsive interactions between positively charged Ca atoms increase with Ca coverage, and at some point, donation of electrons from Ca to Pd is inhibited, and depolarization of Ca−Pd dipoles occurs. The formation of 2D, metallic Ca "rafts" becomes energetically favorable[20] vs separate Ca adatoms, and the surface becomes covered by a mixture of Ca islands and Ca adatom domains in the region of high Ca coverage and eventually is covered by a monolayer of metallic Ca.

The dependence of the saturation CO coverage on the Ca concentration is shown in Figure 10. This CO coverage was calculated from the total area under the CO TPD curves. There are two regions in this curve. The first region at low Ca concentration is determined largely by the van der Waals diameter of the CO molecule and the maximum CO coverage remains close to that obtained for the clean Pd(111) surface. With increasing Ca coverage, however, the number of accessible Pd sites diminishes to such an extent that the surface capacity for CO adsorption drops in proportion to the Ca concentration and goes to zero at 1-ML Ca. The relative decrease in the CO adsorption capacity on Pd(111) for $\Theta_{Ca} = 0.4$ ML is close to the maximum decrease observed upon Ca addition to SiO_2-supported Pd catalysts.

The process of CO adsorption was monitored by using XPS as well. By use of the area of the C(1s) peak, we calculated a saturation CO coverage on the alloy surface of the (2 × 2) Ca/Pd(111) alloy at 320 K of 0.38 ML. This is in reasonable agreement with the results obtained from TPD measurements (0.45 ML). CO monolayer coverage on both clean Pd(111) and the 2 × 2 Ca/Pd(111) alloy resulted in a Pd 3d peak shift to 0.15 eV higher BE. On the alloy, the CO monolayer also resulted in Ca 3p shift of 0.6 eV to higher BE as shown in Figure 11. The Ca 3p peak shift was analyzed by fitting the unresolved Ca doublet with a Gaussian line shape plus an exponential tail. The parameters of this peak shape (except for the height and position) were kept constant during the fitting process. The fact that all the peaks in parts a−d of Figure 11 could be fit with the same, constant full-width half maximum suggests that Ca is present on each surface in a single oxidation state. Figure 11 gives the position of the peak at 24.95 eV BE for an as-deposited 0.33-ML Ca film in which we believe Ca is primarily present as adatoms in the adlayer. When CO was desorbed, the value of this shift decreased to that for a thin Ca overlayer on Pd(111). The change in the position of the Ca 3p peak to higher BE in the presence of CO on the surface and back to lower BE after CO desorption indicates the direct involvement of bonding of Ca to CO. XPS measurements, performed after CO desorption, indicate that Ca is on the surface in a state similar to that of Ca immediately upon deposition. This observation supports the proposal that Ca migrates from the Ca−Pd alloy to the overlayer. This Ca may form an alloy with Pd again if the surface is annealed at the usual temperature required for the alloy formation.

Ca atoms may be driven to the overlayer in two ways. First, they may donate electrons to the Pd, thus increasing its ability to bind CO. This should decrease the C−O bond strength, since Pd will donate more electrons to $2\pi^*$ CO molecular orbitals. Second, as discussed, Ca migration will create a pronounced Ca−Pd interface. In this case, there will be an electrostatic field directed from positively charged Ca atoms to a negatively charged mirror charge plane in Pd, which will lower the energy

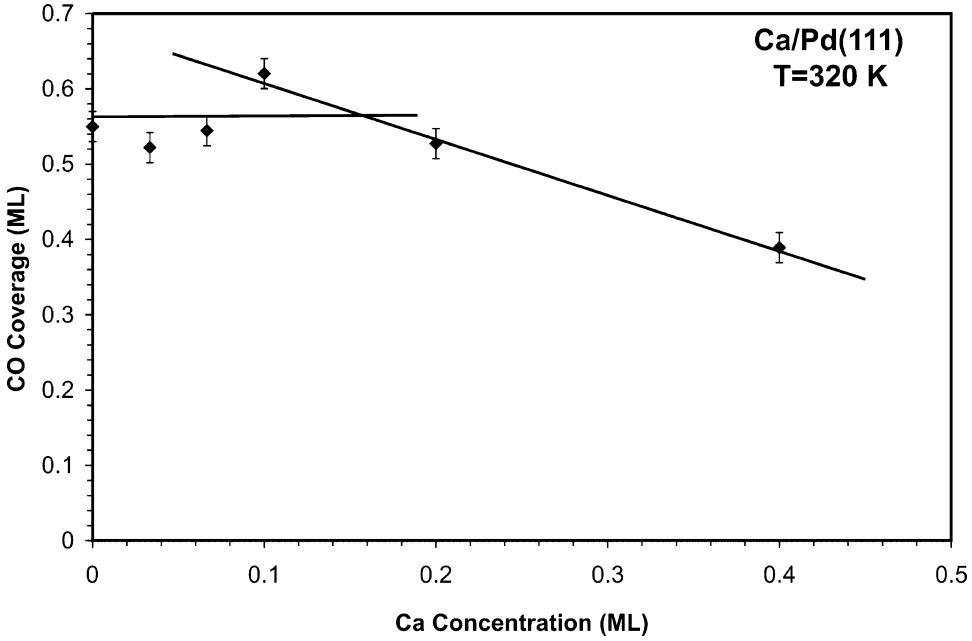

Figure 10. Dependence of the saturation CO monolayer coverage on the Ca coverage on the Pd(111) surface.

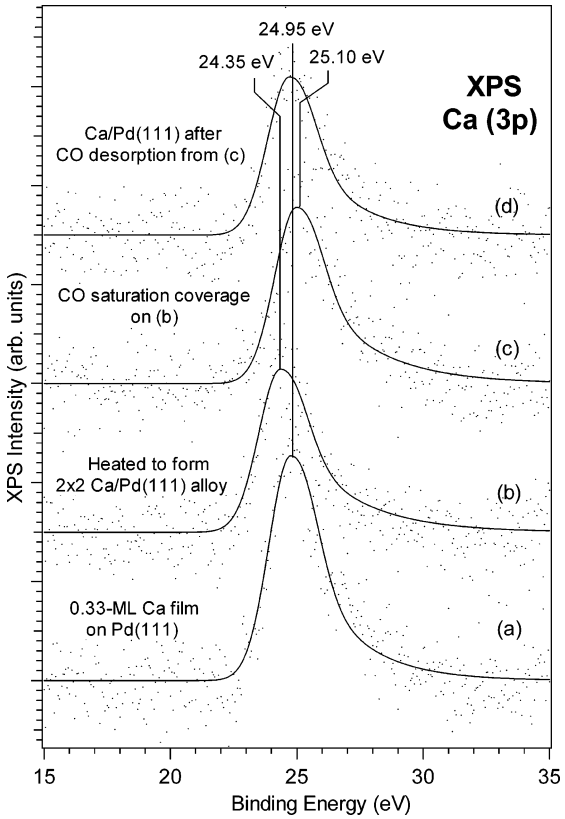

Figure 11. Ca 3p XPS core levels from the (2 × 2) Ca/Pd(111) alloy during CO adsorption−desorption experiments.

of CO molecules on the surface since they have dipole moments oriented in opposite direction.

In discussions of alkali-metal coadsorption with CO on transition-metal surfaces, several models for the alkali−CO interaction have been proposed.[26] These may be divided into direct vs indirect interactions, with the strongest direct interaction leading to compound formation and the weakest indirect interaction providing some through-space electrostatic coupling and/or through-substrate charge-transfer coupling. In a study of a similar system, Li/Ru(001), it was concluded that Li does not form a compound with CO but rather changes the state of the whole Ru surface.[30] We imagine that the chemistry of Ca/Pd(111) is similar and that no Ca−CO compound is formed. It should be possible to rule out or establish such compound formation by performing coverage-dependent vibrational spectroscopy (e.g., infrared reflection absorption spectroscopy or high-resolution electron energy-loss spectroscopy) and other spectroscopic measurements, and we are planning to carry out this type of additional study.

In this work, we made several observations that are relevant to methanol synthesis over Ca-modified, supported Pd catalysts and the nature of the catalytically active phase. First of all, in the high-pressure mixture of CO and H_2 used for this reaction, and in vicinity of metallic Pd particles, which can dissociate hydrogen, there is a good possibility that metallic Ca could be formed in a reducing step during catalyst preparation or under reaction conditions. We have shown that this metallic Ca, if formed in contact with Pd, will readily alloy with Pd at temperatures as low as 700 K. This low temperature of formation and the observed high thermal stability would make such alloys possible candidates for the active phase of these supported Pd−Ca catalysts. However, our observation that adsorption of CO extracts Ca from the substrate to the overlayer at 310 K means that the actual state of Ca on the supported catalyst is still quite uncertain. One must still consider the possibility that Ca would be dealloyed during reaction conditions that generate substantial adsorbate coverages and move to the adlayer. There it could increase the CO adsorption energy, activate the CO bond, and facilitate methanol formation. Second, our observations of strong Pd−Ca bonding and consequent high thermal stability of Ca at Pd surfaces, along with the absence of any Ca−CO co-desorption peak which is common for alkali metal-promoted metal surfaces, may help to explain the special nature of Ca over alkali-metal promoters for this catalysis. Also, strong Pd−Ca bonding results in the formation of several ordered surface alloys with Pd, which is not common for alkali and alkaline-earth metals alloyed with transitional metals. This creates a limited, more-defined set of adsorption and reaction sites at the surface, which could greatly diminish side-product formation.

Conclusion

Pd−Ca alloy surfaces were obtained by deposition of Ca on a Pd(111) single-crystal surface and sequential annealing of the sample to 1100 K. Depending on the initial Ca coverage, this resulted in the formation of a (2 × 2) Ca/Pd(111) or a ($\sqrt{3}\times\sqrt{3}$)R30° Ca/Pd(111) alloy structure. Further annealing of the ($\sqrt{3}\times\sqrt{3}$)R30° Ca/Pd(111) alloy caused conversion of this structure to the (2 × 2) Ca/Pd(111) alloy. Annealing a thick Ca film on Pd(111) caused Ca evaporation from the surface at ∼1100 K, but the (2 × 2) LEED pattern and some remaining Ca was observed even after annealing at 1280 K. This temperature corresponds to a Ca-desorption activation energy of 84 kcal/mol from the(2 × 2) Ca/Pd(111), and so this serves as a lower limit for the Pd−Ca bond energy in this alloy. Thus, Pd−Ca bonding is very strong, and this interaction could stabilize high concentrations of Ca at Pd surfaces in the hydrogenation reaction of CO to methanol over Pd catalysts at the typical reaction temperature of 550 K.

CO adsorption on Ca/Pd alloy surfaces under UHV conditions is a reversible process occurring without oxidation of Ca. The presence of Ca at the Pd(111) surface increases the CO adsorption energy by 7 kcal/mol and causes a 110-K higher temperature CO desorption peak in TPD. The influence of Ca is evident even at low (0.02 ML) Ca coverage. Adsorption of a monolayer of CO on the (2 × 2) alloy at 320 K removed the (2 × 2) LEED pattern as a result of Ca migration to the overlayer, and this was not regenerated by heating to 700 K during TPD. Annealing of this sample at 1000−1100 K caused the reappearance of the (2 × 2) LEED pattern due to realloying of Ca and Pd. Migration of Ca from the alloy to the overlayer creates a network of positively charged Ca atoms, which stabilizes adsorbed CO molecules by electrostatic interactions. In addition, Ca−Pd bonding increases electron density at Pd sites, and this could make Pd a more effective electron donor which would facilitate CO dissociation.

These studies showed that Pd−Ca alloying occurs readily at temperatures above 700 K and that these phases can be ordered surface compounds and quite thermally stable. This makes Pd−Ca alloys possible candidates for the active phase in Ca-modified, supported Pd catalysts for methanol synthesis. However, given that CO adsorption causes dealloying by extraction of surface Ca into the adlayer and the likelihood that functioning Pd−Ca supported catalysts work with significant coverages of adsorbates (at high pressures) under steady-state conditions, it is possible that Ca exists at the surface of Pd metal particles as an overlayer of Ca adatoms rather than alloyed into Pd under reaction conditions. These studies may also help to explain the special nature of Ca over alkali metal promoters for this catalysis, which could be related to the exceptional Pd−Ca bond strength compared to alkali metals.

Acknowledgment. B.E.K. acknowledges support of this work by the Division of Chemical Sciences, Office of Basic Energy Sciences, U.S. Department of Energy.

References and Notes

(1) Tracey, S.; Palermo, A.; Vazquez, J. P. H.; Lambert, R. M. *J. Catal.* **1998**, *179*, 231.
(2) Gotti, A.; Prins, R. *J. Catal.* **1997**, *175*, 302.
(3) Poutsma, M. L.; Elek, L. F.; Ibarbia, P. A.; Risch, A. P.; Rabo, J. A. *J. Catal.* **1978**, *52*, 157.
(4) Rabo, J. A.; Rich, A. P.; Poutsma, M. L. *J. Catal.* **1978**, *53*, 298.
(5) Vannice, M. A. *J. Catal.* **1975**, *37*, 449 and 462.
(6) Ryndin, Y. A.; Hicks, R. F.; Bell, A. T.; Yermakov, Y. I. *J. Catal.* **1981**, *70*, 287.
(7) Fajula, F.; Anthony, R. G.; Lunsford, J. H. *J. Catal.* **1982**, *73*, 237.
(8) Gusovius, A. F.; Watling, T. C.; Prins, R. *Appl. Catal. A* **1999**, *188*, 187.
(9) Lazarev, V. B.; Shaplygin, I. S. *Russ. J. Inorg. Chem.* **1978**, *23*, 1610.
(10) Gerlach, R. L.; Rodin, R. N. *Surf. Sci.* **1970**, *19*, 403.
(11) Surnev, L.; Bliznakov, G.; Kiskinova, M. *Solid State Comm.* **1981**, *37*, 87.
(12) Kiskinova, M.; Surnev, L.; Bliznakov, G. *Surf. Sci.* **1981**, *104*, 240.
(13) Windham, R. G.; Bartram, M. E.; Koel, B. E. *J. Phys. Chem.* **1988**, *92*, 2, 2862.
(14) Somorjai, G. A.; Garfunkel, E. L. In *Physics and Chemistry of Alkali Metal Adsorption*; Elsevier: New York, 1989; 319.
(15) Gusovius, A.; Prins, R. *J. Catal.* **2002**, *211*, 273.
(16) Jerdev, D.; Olivas, A.; Koel, B. E. *J. Catal.* **2002**, *205*, 278.
(17) Powell, C. J.; Jablonsky, A. *Surf. Interface Anal.* **2000**, *29*, 108.
(18) Jiang, L. Q.; Li, Y. D.; Koel, B. E. *Phys. Rev. Lett.* **1993**, *70*, 2649.
(19) Rotenberg, E.; Kevan, S. D. *Advanced Light Source: Compendium of User Abstracts and Technical Reports*, 1997; LBL-41658, UC-411; LBL: Berkeley, 1998; pp 114−115.
(20) Naumovets, A. G.; Vedula, Yu. S. *Surf. Sci. Reports* **1985**, *129*, 365.
(21) Doering, D. L.; Semancik, S. *Surf. Sci.* **1983**, *129*, 177.
(22) Besold, G.; Schaffroth, Th.; Heinz, K.; Schmidt, G.; Muller, K. *Surf. Sci.* **1988**, *194*, 159.
(23) Pirug, G.; Bonzel, H. P. *Surf. Sci.* **1988**, *194*, 159.
(24) Chandavarkar, S.; Dehl, R. D. *Phys. Rev. B* **1988**, *38*, 12112.
(25) Michaelson, H. B. *J. Appl. Phys.* **1977**, *48*, 4731.
(26) Naumovets, A. G. *Surf. Sci.* **1994**, *299*, 706.
(27) Habenschaden, E.; Kuppers, J. *Surf. Sci.* **1984**, *L147*, 138.
(28) Kittel, C. *Introduction to Solid State Physics*, 7th ed.; Wiley: New York, 1996.
(29) de Boer, F. R.; Boom, R.; Mattens, W. C. M.; Miedema, A. R.; Niessen, A. K. In *Cohesion in Metals, Transition Metal Alloys*; Elsevier: New York, 1988; p 479.
(30) Jansch, H. J.; Polenz, C.; Bromberger, C.; Detje, M.; Ebinger, H. D.; Polivka, B.; Preyss, W.; Veith, R.; Fick, D. *Surf. Sci.* **2001**, *495*, 120.
(31) Netzer, F. P.; Doering, D. L.; Madey, T. E. *Surf. Sci.* **1984**, *143*, 83.
(32) Hoffmann, F. M.; Hrbek, J.; DePaola, R. A. *Chem. Phys. Lett.* **1984**, *106*, 83.
(33) Weimar, J. J.; Umbach, E.; Menzel, D. *Surf. Sci.* **1985**, *155*, 132.
(34) Erley, W.; Wagner, H. *J. Chem. Phys.* **1980**, *72*, 2207.
(35) Kiskinova, M.; Bliznakov, G. *Surf. Sci.* **1982**, *123*, 61.
(36) Wandelt, K. In *Physics and Chemistry of Alkali Metal Adsorption*; Elsevier: New York, 1989; p 25.